JOURNAL OF CATALYSIS 2, 69–78 (1963)

Fourier Peak-Shape Analyses of Catalyst Iron and Cold-Worked Iron*

F. H. HERBSTEIN AND JACQUES SMUTS†

From the National Physical Research Laboratory, Council for Scientific and Industrial Research, Pretoria, South Africa

Received September 11, 1962

Peak broadening in X-ray diffraction patterns of reduced Fischer-Tropsch iron catalysts has been analyzed by the Fourier method. The results show that the observed peak broadening is due to the combined effects of small crystallite sizes, faulting on (211) planes, and lattice strains. These quantities are discussed in terms of the methods of preparation of the samples and their catalytic behavior. Similar analyses for cold-worked iron (filed and ground) gave results in agreement with those of Wagner (*5*).

1. INTRODUCTION

α-Iron, produced by reduction of fused magnetite, is used as catalyst in both the Fischer-Tropsch process for the catalytic hydrogenation of carbon monoxide (*1*) and the Haber ammonia synthesis (*2*). It is of interest to compare the catalytic behavior of α-iron samples prepared in different ways and this has been done, for the Fischer-Tropsch process, for the two samples described below (Section 2). The differences in catalytic behavior could not be explained by plant factors and composition alone and attention was therefore directed to the structural features of the samples. Preliminary work showed different degrees of peak broadening in the X-ray powder patterns of the two samples. It was therefore decided to apply the Fourier method of peak-shape analysis (*3*) to obtain a detailed physical picture of the state of the samples. Although the Fourier method has been widely applied in the last thirteen years to studies of cold-worked metals, it has not been used to study other types of sample; peak breadths have, however, been used by Nielsen (*4*) to investigate various ammonia catalysts. Study of peak shapes should give more detailed results than can be obtained from peak breadths alone.

At the same time two cold-worked samples were also examined. These were a sample of iron filings, in order to compare the present results with those of Wagner (*5*) as a check on the reproducibility of the method, and a sample of ground iron which had been used for measurement of the Debye temperature (*6*).

2. CHOICE OF SAMPLES

Reduced Catalyst Samples

The two α-iron catalyst samples which differed markedly in their catalytic properties and which originated the study, were prepared and tested as follows by SASOL staff at Sasolburg:

Singly reduced fused magnetite (hereafter referred to as S.R.F.M.) was obtained by reduction with hydrogen of fused promoted magnetite. The promoters consisted of silica and alumina present as impurities ($\sim$1%) in the Alanwood ore and potassium added as a chemical promoter. Reduction was carried out at about 380°C after

* Research supported by the South African Coal, Oil and Gas Corporation (SASOL).

† Present address: S. A. Iron and Steel Corporation, Pretoria, South Africa.

the fused magnetite had been crushed and ground to a convenient particle size.

Triply reduced catalyst (hereafter referred to as T.R.C.) was treated in the same way as S.R.F.M. except that it had been used twice as catalyst in a synthesis reactor and had been reduced at 380°C each time after use. The following differences were observed between S.R.F.M. and T.R.C. before the peak-shape analyses were carried out.

(a) S.R.F.M. showed a higher initial activity than T.R.C.

(b) The decline in activity for S.R.F.M. was faster than for T.R.C., i.e. the latter was a more stable catalyst.

(c) T.R.C. contained about 4% free carbon whereas S.R.F.M. did not contain any free carbon. Both samples contained traces of unreduced magnetite.

(d) The reduction time for S.R.F.M. was about three times as long as for T.R.C.

(e) The particle size of S.R.F.M. was about double that of T.R.C. (The particle size should not be confused with the crystallite size, which is the size of the coherently diffracting domains.)

(f) The Bragg reflections of S.R.F.M. were broadened to a larger extent than those of T.R.C. This can be seen from Fig. 1 where the peak profiles of the (211) reflection of α-iron are compared for some of the samples.

In addition to the above-mentioned catalyst samples a few others were also examined. These were prepared by Mr. F. R. Maritz at the National Chemical Research Laboratory, Pretoria. A sample of unfused magnetite was reduced at 480°C. The Bragg reflections of the α-iron obtained showed very little broadening. Part of this sample (R.M.) was nitrided and then carbided before it was reduced again at 480°C. For this sample the degree of peak broadening was practically the same as for the reduced magnetite so that it was not considered for further analysis.

In order to allow direct comparison of R.M. with S.R.F.M. and T.R.C., portions of the latter two samples were annealed for 24 hours at 480°C in a nitrogen atmosphere and peak-shape analyses carried out.

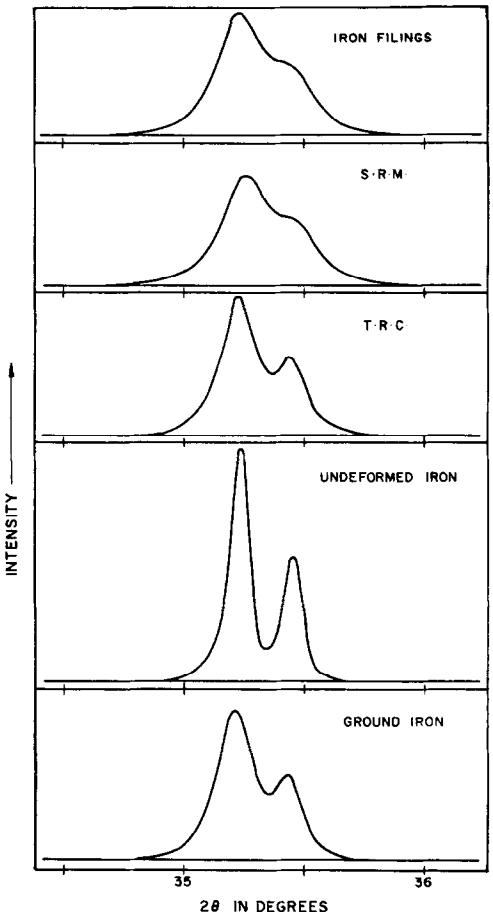

FIG. 1. Profiles of the (211) peak of α-iron (Mo-$K\alpha$ radiation) for various α-iron samples.

Cold-Worked Samples

Iron filings were obtained at room temperature from a Specpure iron rod (Johnson and Matthey). The ground sample was obtained by grinding a −400 mesh ($<38\ \mu$) portion of a well-crystallized iron powder (Riedel de Haen) for 5 hours in a mechanical mortar under benzene. The Bragg reflections were broadened but not as much as those of the iron filings.

3. GENERAL OUTLINE OF METHOD

The X-ray diffraction methods used for the derivation of information about the physical state of a sample from its powder pattern have been comprehensively discussed by Warren (*3*). The following brief

outline of the main features of these methods may be useful to readers unacquainted with them; for details Warren's review should be consulted.

The Bragg reflections from a deformed sample will be broadened due to two physical effects. Firstly the crystallite size may be small enough for the Laue interference function maxima to be broadened; this broadening will be the same for all points of the reciprocal lattice. (A crystallite is defined as a region or domain within which coherent diffraction occurs. Its size may vary in different $[hkl]$ directions and is denoted by $L(hkl)$ in the present paper but by $D(hkl)$ by Warren. Note that we use "crystallite" where Warren uses "particle"; domain is synonymous with crystallite here but with particle in Warren's review.) Secondly there may be broadening due to strains in the crystallite. Here one may roughly consider the reciprocal lattice of the crystallite to be formed by superposition of a number of reciprocal lattices of different dimensions derived from the regions of varying strain in the crystallite. The broadening of the reflections due to strain will vary with their position in reciprocal space. The R.M.S. strain in the $[hkl]$ direction is defined as

$$\langle(\epsilon_L(hkl))^2\rangle^{1/2} = \langle(\Delta L/L(hkl))^2\rangle^{1/2}$$

where ΔL is the deviation of the actual length of a column of unit cells in the $[hkl]$ direction from that of an unstrained column of length L. The average is taken over all crystallites in the sample and, with powdered samples, over all symmetry-related $[hkl]$ directions.

There may also be stacking faults in the crystallite. In face-centered cubic crystals the sequence of (111) planes can be changed from the normal ABCABC to ABCACABC (deformation fault) or ABCACBA (growth or twin fault). In body-centered cubic crystals, such as α-iron, the faults occur on (211) planes but the situation is somewhat more complex than in FCC crystals and reference should be made to Warren for details. The probability of a deformation fault is given by α where $1/\alpha$ is the average number of layers between two deformation faults; the probability of a growth fault, β, is defined in an analogous way. Faulting has three effects on the diffraction pattern: firstly there is a broadening similar to that arising from small coherently diffracting domains; secondly there can be peak shifts and, thirdly, peak asymmetries. The combined effects of domain size ($\bar{L}$), deformation-fault probability (α), and growth-fault probability (β) are derived from the apparent or effective measured crystallite size $[L_E(hkl)]$ which is obtained from the peak broadening; α can be obtained independently from the peak shifts and β from the peak asymmetries. In FCC crystals independent values of the quantities $\bar{L}$ (the true domain size), α, β, and R.M.S. strain $\langle\epsilon_L^2\rangle^{1/2}$ can be obtained from measurements of peak shapes and peak shifts. In BCC crystals the peak shifts due to the various reflection components superimposed in the powder pattern cancel, while the peak asymmetries are considered to be too small to measure. Thus only the combined effects of $\bar{L}$, α, and β can be obtained from measurements of peak broadening [see Eqs. (1) and (2)]. In some BCC crystals it is found that the values of $L_E(hkl)$ derived from different reflections differ considerably. If the crystallite-size broadening were due entirely to faulting then $L_E(110):L_E(200):L_E(211) = 2.83:1:1.63$. Alternatively, if faulting were of no importance and the domains were isotropic, this ratio would be unity. In practice faulting on (211) planes provides a natural explanation for any anisotropy found experimentally in $L_E(hkl)$. The assumption is made that the true domains are isotropic.

Crystallite-size broadening can be distinguished from strain broadening by using two (or more, if available) orders of a given reflection because these two types of broadening depend differently on position in reciprocal space. The description of the peak shapes by Fourier series allows a much more reliable separation of these two effects than did the earlier methods which relied on peak breadths rather than peak shapes.

4. Experimental Procedure

Peak profiles of the (110), (200), (211), (220), (400), and (422) reflections of α-iron were obtained for all the samples with a Philips PW 1050 X-ray diffraction unit. Samples for the diffractometer were packed from the front in ordinary glass sample holders, only specimens with particle size smaller than 38 μ being used. Profiles for the (110), (200), (211), and (220) reflections were recorded automatically on diffractometer charts using Fe-filtered Co $K\alpha$ radiation, care being taken not to exceed a counting rate of 400 counts per second for the argon-filled Geiger counter. The weaker reflections, (400) and (422), were recorded by automatic point-by-point counting (*7*) (Kr-filled Geiger counter) using Zr-filtered Mo $K\alpha$ radiation. Angular intervals between points varied from 1/16° 2 θ at background positions to 1/64° 2 θ at peak positions.

Unbroadened profiles were determined from the well-crystallized iron powder used later to prepare the ground sample. Before grinding this powder had a mean crystallite size of 5 μ [measured by Warren's method (*8*)]. Care was taken to use the same experimental conditions as for the recording of the broadened profiles. Each peak profile was divided into a large number of intervals to suit the divisions on the recorder charts. The origin was always taken at the peak maximum. Errors introduced by small peak shifts were eliminated by assuming symmetrical diffraction broadening in each case. The correct Fourier coefficients A_n could therefore be calculated from the real and imaginary parts, A_n' and B_n', of the coefficients for the misplaced peaks, the relation used being $A_n = (A_n'^2 + B_n'^2)^{1/2}$ (*9*). Experiment showed that peak shifts of up to 15% of the total Fourier interval of a broadened profile did not change the values of A_n. The Fourier coefficients were corrected for instrumental broadening by Stokes' method (*10*), all the computations being done by a Zebra electronic computer.

The effects of crystallite size and lattice strains were separated by using Warren and Averbach's method (*11*). The frequency numbers, n, were converted to distances L so that the calculated crystallite-size components A_L^c of the Fourier coefficients A_L, could be plotted directly against L. These were corrected for the "hook effect" (*12*) and the average effective crystallite sizes read off at the intercepts with the abscissa of the initial slopes of the A_L^c vs. L curves. Values for the root mean square lattice strain $\langle \epsilon_L^2 \rangle^{1/2}$ were calculated for different values of L from the curves of $\ln A_L$ against $(h^2 + k^2 + l^2)$.

Faulting probabilities and true crystallite sizes were calculated from the effective

TABLE 1

Measured Crystallite Sizes for Different α-Iron Samples

Sample	Measured crystallite size (Å)		
	$L_E(110)$	$L_E(200)$	$L_E(211)$
1. Singly reduced fused magnetite (S.R.F.M.)	250	175	200
	280[a]	—	—
2. S.R.F.M. annealed 24 hours at 480°C	260	190	240
3. Triply reduced catalyst (T.R.C.)	340	250	280
	330[a]	—	—
4. T.R.C. annealed 24 hours at 480°C	430	—	370
5. Reduced unfused magnetite (R.M.)	800	1100	700
6. Iron filings (present work)	280	155	160
7. Iron filings (Wagner)	280	140	170
8. Iron filings annealed 1 hour at 265°C (Wagner)	600	360	460
9. −400 mesh iron powder ground for 5 hours under benzene	550	250	390

[a] The second value was obtained from a different set of measurements.

crystallite sizes in the [110], [100], and [211] directions using the relations given by Guentert and Warren (*13*), i.e.

$$\frac{1}{L_E} = \frac{1}{L_F} + \frac{1}{\bar{L}} \tag{1}$$

$$\frac{1}{L_F}(110) = \frac{\sqrt{2}(1.5\alpha + \beta)}{3a}$$

$$\frac{1}{L_F}(100) = \frac{4(1.5\alpha + \beta)}{3a} \tag{2}$$

$$\frac{1}{L_F}(211) = \frac{\sqrt{6}(1.5\alpha + \beta)}{3a}$$

in which L_F is a fictitious crystallite size due to stacking faults, L_E is the measured crystallite size, $\bar{L}$ is the true crystallite size, and $(1.5\,\alpha + \beta)$ combines the probabilities for the occurrence of deformation and twin faults. Equations like (1) were set up for each crystallographic direction and solved in pairs for $\bar{L}$ and $(1.5\,\alpha + \beta)$.

5. Results

The results of the analyses are presented in Tables 1, 2, and 3 together with the results obtained by Wagner for iron filings. The measured crystallite sizes and strain values are given in Tables 1 and 3 while Table 2 gives the values for true crystallite sizes and faulting probabilities. Since the two samples prepared from unfused magnetite showed very little difference in the degree of peak broadening only one of them, reduced magnetite, was used for peak-shape analysis. The degree of peak broadening for this sample was very small so that accurate results could not be obtained and for this reason values of the true crystallite size and faulting probabilities are not given.

No obvious straight line could be drawn through the points of the plot of $A_L{}^c$ vs. L for the [100] direction in the annealed specimen of T.R.C. so that no reliable figure could be obtained for $L_E(200)$ for this sample.

The results of duplicate analyses for the [110] direction are included for S.R.F.M. and T.R.C. In this case Lipson-Beevers strips were used for the calculation of Fourier coefficients.

TABLE 2

True Crystallite Sizes and Faulting Probabilities for Different α-Iron Samples

Sample	Calculated true crystallite sizes $\bar{L}$ (Å)				Faulting probabilities $(1.5\alpha + \beta)$			
	(110)–(200)	(110)–(211)	(200)–(211)	Mean	(110)–(200)	(110)–(211)	(200)–(211)	Mean
1. S.R.F.M.	327	380	258	320	.006	.008	.004	.006
2. S.R.F.M. annealed	325	293	408	340	.005	.003	.006	.005
3. T.R.C.	424	452	346	410	.004	.005	.002	.004
4. T.R.C. annealed	—	546	—	550	—	.003	—	.003
5. R.M.	—	—	—	—	—	—	—	—
6. Filings (present work)	500	∞	156	See Sect. 6 of text	.010	.022	.001	See Sect. 6 of text
7. Filings (Wagner)	—	—	—	600	—	—	—	.012
8. Filings annealed (Wagner)	—	—	—	1000	—	—	—	.004
9. Ground iron	1590	1230	2630	1800	.007	.006	.008	.007

TABLE 3
ROOT MEAN SQUARE STRAINS

	Crystallographic direction	Values of R.M.S. strain $\langle \epsilon^2 \rangle^{1/2} \times 10^3$					
		L = 25 Å	50 Å	75 Å	100 Å	125 Å	150 Å
1. S.R.F.M.	110	3.4	2.6	2.1	1.8	1.6	1.4
	200	3.9	3.1	2.6	2.3	2.0	1.7
	211	2.9	2.2	1.9	1.6	1.4	1.3
2. S.R.F.M. annealed	110	1.0	1.1	1.2	1.3	1.4	1.3
	200	—	4.1	3.0	2.2	—	—
	211	—	2.2	1.8	1.5	1.3	1.1
3. T.R.C.	110	2.3	2.0	1.7	1.5	1.3	1.1
	200	2.8	2.2	1.8	1.6	1.4	1.2
	211	2.4	1.7	1.4	1.2	1.1	1.0
4. T.R.C. annealed	110	1.4	1.3	1.2	1.0	0.9	0.8
	200	—	3.4	2.6	2.1	—	—
	211	—	1.8	1.4	1.1	1.0	0.9
5. R.M.	110	—	0.8	0.8	0.8	0.7	0.7
	200	—	—	—	—	—	—
	211	—	—	—	—	—	—
6. Iron filings (present work)	110	3.4	3.1	2.5	2.2	2.0	1.8
	200	4.1	3.5	3.1	2.9	2.6	—
	211	3.0	2.2	1.9	1.8	1.7	1.6
7. Iron filings (Wagner)	110	—	2.5	—	2.0	—	—
	200	—	3.1	—	2.4	—	—
	211	—	2.0	—	1.6	—	—
8. Iron filings annealed (Wagner)	110	—	1.2	—	—	—	—
	200	—	1.7	—	—	—	—
	211	—	1.0	—	—	—	—
9. Ground iron	110	—	2.2	1.8	1.6	1.4	1.3
	200	—	2.2	1.8	1.6	1.4	1.3
	211	—	1.7	1.5	1.3	1.2	1.1

6. RELIABILITY OF THE RESULTS

From a comparison of the present results for iron filings with those obtained by Wagner and also from the results of duplicate analyses, it can be concluded that the measured crystallite sizes are accurate to about 10%. However, there are cases where results should be interpreted with care, e.g. the values for the [100] direction for S.R.F.M. and iron filings. The (400) reflection of α-iron is very weak and falls between two much stronger reflections, (321) and (411, 330), so that its shape can be influenced by the tails of these stronger reflections if the degree of peak broadening is large. This is illustrated for iron filings in Fig. 2. It can be seen clearly that the shape of the (400) reflection is markedly influenced by the tails of the strong neighboring reflections. This applies also for S.R.F.M. In addition to this interference the accuracy is also limited by the low intensity.

The results for true crystallite sizes and faulting probabilities should also be interpreted with care since the values of these quantities are very sensitive to small variations in the measured crystallite sizes. The following should serve as an example. The values obtained for iron filings differed

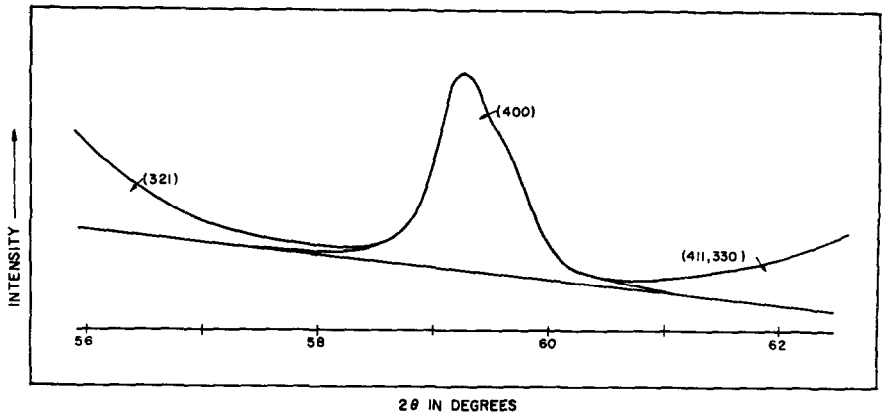

FIG. 2. Illustration of the overlapping effect of the tails of the (321) and (411, 330) reflections on the shape of the (400) reflection for iron filings (Mo $K\alpha$ radiation).

widely (see Table 2); however, if the values of L_E are all changed by about 10% so that $L_E(110) = 252$ Å, $L_E(200) = 140$ Å, and $L_E(211) = 186$ Å, the following results will be obtained:

Line pair	$\bar{L}$ in Å	$1.5\alpha + \beta$
(110)–(200)	452	.011
(110)–(211)	489	.012
(200)–(211)	387	.010
Mean	443 ± 35	.011 ± .001

These values agree much more closely than do those given in Table 2.

7. Discussion

Summary

The following comparative summary of the results has been prepared to facilitate interpretation:

(*i*) S.R.F.M. has a smaller mean crystallite size and larger lattice strains than T.R.C. On the other hand these quantities are of the same magnitude for S.R.F.M. and iron filings. Faulting probabilities for S.R.F.M. are smaller than those for iron filings which means that the latter has a larger true crystallite size.

(*ii*) In reduced unfused magnetite (R.M.) the crystallites are large and isotropic in size in contrast to the small anisotropic crystallite sizes observed for reduced fused magnetite (S.R.F.M.).

(*iii*) Annealing of S.R.F.M. and T.R.C. (24 hours at 480°C) resulted in some crystal growth and lowering of strain values but the mean crystallite sizes were still much lower and the strain values higher than those of R.M. The changes that occurred during annealing were also much less marked than those occurring when iron filings were annealed for a much shorter time at a much lower temperature (1 hour at 265°C) (*5*). S.R.F.M. was influenced to a smaller extent by annealing than T.R.C.

(*iv*) The crystallites in iron filings were deformed much more than those of the ground iron—the crystallite size of the former is smaller, the r.m.s. lattice strains larger and the faulting probability larger.

The experimental results for the samples obtained by reduction are qualitatively similar to those reported by previous workers. Wyckoff and Crittenden (*14*) showed many years ago that iron powders obtained by reduction of promoted, fused magnetite were little affected by annealing conditions that produced appreciable crystal growth in pure iron. Nielsen (*4*) concluded, from peak-breadth analyses, that the peak broadening from iron-ammonia catalysts was due to small crystallite size alone, and obtained a crystallite size of 360 Å. This value is not too different from the $L_E(hkl)$ values obtained in the present investigation for S.R.F.M. and, particularly, T.R.C. However, the Fourier analyses show that strain broadening and faulting also con-

tribute to the peak profiles found experimentally.

There are a number of relevant factors which, for convenience, will be discussed separately in the explanation of the observed physical differences among the samples examined. It should, however, be remembered that these factors may be closely connected.

The Effect of Structural Promoter and the Method of Preparation on the Physical State of a Catalyst

It is generally believed that the action of a structural promoter on a catalyst is to create a large surface (*14*), i.e a small crystallite size, and to preserve this large surface, i.e. to prevent crystal growth. In order to create a small crystallite size, the structural promoter should be distributed well. It should also consist of a material which is inactive so that it cannot be removed from the interfaces of the crystallites. The behavior of alumina as structural promoter is explained as follows. Alumina goes into solid solution in magnetite (Fe_3O_4) when the two substances are fused together, the aluminum atoms then being distributed essentially at random in the magnetite lattice. On reduction of the magnetite the alumina separates out between the α-iron crystallites in the form of thin layers which are barriers to crystal growth. Small concentrations of alumina are sufficient to accomplish this. This situation has been demonstrated electron microscopically for magnetite singly promoted with alumina (*15, 16*). Although the composition of the present samples is more complex, the same general picture should apply and the discussion below has been worded in terms of an intercrystalline film nominally composed only of alumina.

Both the effect of alumina and of sample origin are clearly illustrated by the results of the Fourier analyses. All the reduced samples contained about the same amount of alumina (about 0.6%). Only one of them, S.R.F.M., had been fused immediately before reduction and this sample had by far the smallest crystallite size. This illustrates the effect of the alumina layers in preventing growth of the iron crystallites. The other catalyst, T.R.C., had been used twice after fusion and reduction so that the original distribution of the intercrystalline films must have changed appreciably and these were no longer as effective in retarding the growth of the iron crystallites. Therefore the crystallite size of T.R.C. is larger than that of S.R.F.M. The smaller effect of annealing (24 hours at 480°C) on S.R.F.M. than on T.R.C. is also attributable to the difference in the distribution of intercrystalline films. In the case of R.M. the magnetite had not been fused, alumina had not gone into solid solution and consequently large crystallites were obtained on reduction. Similarly the filings examined by Wagner (*5*) were of pure iron and thus crystal growth could take place much more easily than in the promoted samples, despite the relatively short annealing time and low annealing temperature used.

All samples except R.M. show anisotropic crystallite sizes and this has been interpreted (*5, 13*) as due to faulting on (211) planes. As the catalyst samples were not deformed it seems probable that, for them, these are mainly growth (twin) faults. The different situation in R.M. suggests either that the twins anneal out in fairly large crystallites, or that the intercrystalline film has some influence on the incidence of twins.

Catalytic Properties

The difference in catalytic behavior between S.R.F.M. and T.R.C. can be partially explained in terms of the results obtained in this work and their compositions. The higher activity of S.R.F.M. is in direct agreement with its smaller crystallite size since activity is *inter alia* proportional to surface area which is inversely proportional to crystallite size. It is reasonable to assume that in a reduced catalyst the grain boundaries are mainly formed by layers of structural promoter so that the surface area is to a large extent determined by the crystallite size.

From the work of Westrik and Zwieter-

ing (*17*) it appears that the nature of the precatalyst before reduction can have a marked effect on the catalytic properties of the reduced material. Magnetite gives an active catalyst on reduction for the following reasons: magnetite crystals show a preference to be bounded by (111) planes. On reduction the α-iron crystallites formed also show a preference to be bounded by (111) planes, which, according to Beeck *et al.* (*18*), are the most active faces (of α-iron) for chemisorption of carbon monoxide. The higher observed activity of S.R.F.M. is also in agreement with the above since the precatalyst consisted mainly of magnetite whereas T.R.C. was prepared by reduction of a material rich in iron carbides. These carbides have complex structures so that it is doubtful that they will give on reduction a material with the same face development as reduced magnetite.

The effect of free carbon on the properties of a catalyst has not yet been well established. According to Stein *et al.* (*19*) it can have a stabilizing effect. This is in agreement with the higher stability of T.R.C. which contained about 4% free carbon. The most probable picture here is that the inactive free carbon acts in a similar way to the structural promoter, i.e. provides an open structure and prevents crystal growth.

The presence of lattice strains in S.R.F.M. and T.R.C. was unexpected since both samples had been reduced at 380°C. Further annealing at a higher temperature (480°C) did not cause these strains to disappear. Their presence might perhaps be coupled with the crystallite size in such a way that their magnitude is inversely proportional to the crystallite size. The behavior of the catalyst samples on annealing is in agreement with such an hypothesis.

The smaller particle size of T.R.C. compared to S.R.F.M. is probably due to the more severe mechanical and chemical treatment it had received in the synthesis reactor, while the difference in reduction rates is probably a consequence of the different chemical compositions of the samples before reduction [see Clarke, Dry, and van Zyl (*20*) for discussion and earlier references].

Cold-Worked Samples

The results for iron filings agree, within the limits of error, with those obtained by Wagner and his discussion will not be repeated here. The results for the ground iron sample show a similar pattern but the quantitative differences between filed and ground samples are due to the less severe deformation in the latter.

Acknowledgments

We are indebted to Drs. J. D. Louw and L. J. Dry and Mr. F. R. Maritz for samples, to Dr. J. N. van Niekerk for his interest in this work and to Dr. J. D. Neethling for the Zebra computer program. One of us (J. S.) used this work as part of a doctoral thesis at the University of Stellenbosch. We are also grateful to the South African Coal, Oil and Gas Corporation for provision of facilities and permission to publish these results.

References

1. Pichler, H., *Advances in Catalysis* **4**, 272 (1952).
2. Nielsen, A., *Advances in Catalysis* **5**, 1 (1953).
3. Warren, B. E., *Prog. in Metal Phys.* **8**, 147 (1959).
4. Nielsen, A., "An Investigation on Promoted Iron Catalysts for the Synthesis of Ammonia," 2nd ed., Jul. Gjellerups Forlag, Copenhagen, 1956.
5. Wagner, C. N. J., *Arch. Eisenhüttenw.* **29**, 489 (1958).
6. Herbstein, F. H., and Smuts, Jacques, to appear in *Phil. Mag.*, 1963.
7. Schroeder, W. W., in preparation.
8. Warren, B. E., *J. Appl. Phys.* **31**, 2237 (1960).
9. Schoening, F. R. L., *Acta Met.* **4**, 510 (1956).
10. Stokes, A. R., *Proc. Phys. Soc. London* **61**, 382 (1948).
11. Warren, B. E., and Averbach, B. L., *J. Appl. Phys.* **23**, 497 (1952).
12. Despujols, J., and Warren, B. E., *J. Appl. Phys.* **29**, 195 (1958).
13. Guentert, O. J., and Warren, B. E., *J. Appl. Phys.* **29**, 40 (1958).
14. Wyckoff, R. W. G., and Crittenden, E. G., *J. Am. Chem. Soc.* **44**, 2286 (1925).
15. Schäfer, K., *Z. Elektrochem.* **64**, 1190 (1960).
16. Peters, Cl., Schäfer, K., and Krabetz, R., *Z. Elektrochem.* **64**, 1194 (1960).

17. WESTRIK, R., AND ZWIETERING, P., *Proc. Nederlandse Akad. Wetenschappen* **56,** 492 (1953).

18. BEECK, O., WHEELER, A., AND SMITH, A. E., *Phys. Rev.* **55,** 601 (1939).

19. STEIN, K. C., THOMPSON, G. P., AND ANDERSON, R. B., *J. Phys. Chem.* **61,** 928 (1957).

20. CLARKE, J. J., DRY, M. E., AND VAN ZYL, W. J., *J. S. African Chem. Inst.* **15,** 11 (1962).